

A discrete mathematical model for the dynamics of a crowd of gazing pedestrians with and without an evolving environmental awareness

*Original*

A discrete mathematical model for the dynamics of a crowd of gazing pedestrians with and without an evolving environmental awareness / Colombi, Annachiara; Scianna, Marco; Alaia, Alessandro. - In: COMPUTATIONAL AND APPLIED MATHEMATICS. - ISSN 0101-8205. - 36:2(2017), pp. 1113-1141. [10.1007/s40314-016-0316-x]

*Availability:*

This version is available at: 11583/2644674 since: 2018-03-06T14:34:29Z

*Publisher:*

Birkhauser Boston Incorporated:c/o Springer Verlag

*Published*

DOI:10.1007/s40314-016-0316-x

*Terms of use:*

This article is made available under terms and conditions as specified in the corresponding bibliographic description in the repository

*Publisher copyright*

Springer postprint/Author's Accepted Manuscript

This version of the article has been accepted for publication, after peer review (when applicable) and is subject to Springer Nature's AM terms of use, but is not the Version of Record and does not reflect post-acceptance improvements, or any corrections. The Version of Record is available online at: <http://dx.doi.org/10.1007/s40314-016-0316-x>

(Article begins on next page)

# A discrete mathematical model for the dynamics of a crowd of gazing pedestrians with and without an evolving environmental awareness

Annachiara Colombi · Marco Scianna ·  
Alessandro Alaia

Received: date / Accepted: date

**Abstract** In this article, we present a microscopic-discrete mathematical model describing crowd dynamics in no panic conditions. More specifically, pedestrians are set to move in order to reach a target destination and their movement is influenced by both behavioral strategies and physical forces. Behavioral strategies include individual desire to remain sufficiently far from structural elements (walls and obstacles) and from other walkers, while physical forces account for interpersonal collisions. The resulting pedestrian behavior emerges therefore from non-local, anisotropic and short/long-range interactions. Relevant improvements of our mathematical model with respect to similar microscopic-discrete approaches present in the literature are: i) each pedestrian has his/her own dynamic gazing direction, which is regarded to as an independent degree of freedom and ii) each walker is allowed to take dynamic strategic decisions according to his/her environmental awareness, which increases due to new information acquired on the surrounding space through their visual region. The resulting mathematical modeling environment is then applied to specific scenarios that, although simplified, resemble real-word situations. In particular, we focus on pedestrian flow in two-dimensional buildings with several

---

A. Colombi  
Department of Mathematical Sciences, Politecnico di Torino, Corso Duca degli Abruzzi 24,  
10129, Torino, Italy  
Tel.: +39 011 564 7558  
E-mail: annachiara.colombi@polito.it

M. Scianna  
Department of Mathematical Sciences, Politecnico di Torino, Corso Duca degli Abruzzi 24,  
10129, Torino, Italy  
Tel.: +39 011 564 7558  
E-mail: marcosci1@alice.it

A. Alaia  
Optimad Engineering, Via G. Collegno 18, 10143, Torino, Italy  
Tel.: +39 011 197 19 782  
E-mail: alessandro.alaia@optimad.it

structural elements (i.e., corridors, divisors and columns, and exit doors). The noticeable heterogeneity of possible applications demonstrates the potential of our mathematical model in addressing different engineering problems, allowing for optimization issues as well.

**Keywords** crowd dynamics · evacuation · environmental awareness · gazing direction · social and physical forces

## 1 Introduction

Collective phenomena observed in human crowds both in normal and in panic conditions has been addressed by a rapidly increasing number of multidisciplinary approaches. Particularly engaging and challenging is the self-emergence of ordered and coordinated configurations from apparently uncorrelated pedestrian dynamics (for example, segregation of opposite flows in pedestrian counter-streams [50], turbulent movement in extremely dense crowds [65], or pattern formation around bottleneck structural elements [27], [41], [49]). In fact, such group organizations are not the result of a common decision made by all individuals or by a leader, rather, they stem from simple sociological and behavioral rules followed by each person, who probably does not even perceive the global structure of the crowd he/she is part of.

For decades, pedestrian crowds have been studied with empirical approaches only, as the evaluation methods have been typically based on direct observation, photographs and time-lapse movies, see for example [4], [15], [25], [40], [58]. These methodologies have been able to collect a large amount of data regarding a wide range of pedestrian walking determinants, such as mean speeds and preferential directions, reactions to the presence of obstacles and/or attraction points, individual behavior in fog or in dangerous situations, thereby providing an important *descriptive* value. However, they have not been satisfactory from a *predictive* point of view.

In relatively recent years, traditional methods to investigate crowd dynamics increasingly integrate and interface with computational approaches deriving from applied physics, mathematics and engineering. Computer simulations can firstly provide a powerful tool for designing and planning urban infrastructures, such as crowd facilities, subway or railway stations, stadia, pedestrian precincts, shopping malls, or big buildings. In fact, they can be used for a preliminary study, in order to test different design solutions, as well as for optimization issues. Moreover, virtual simulations are able to highlight critical conditions in which crowd disasters may occur and suggest effective countermeasures to improve safety of mass events. The underlying requirement is obviously that theoretical models must be accurate enough to catch complex unsteady crowd dynamics but also versatile and able to deal with different real-world applications. To this purpose, modeling pedestrian dynamics is a difficult task because modelers have to take into account that a human crowd, as other complex living systems such as groups of animals [48], is a

*complex system*. In fact, walking individuals are not *passively* dragged by external forces but undergo *active* decision-based dynamics so that the use of the well-established classical passive mechanics is no longer sufficient.

As nicely reviewed in [29], [61], the early computational methods of pedestrian flows date back to more than forty years ago and include models for queuing and route choice [53], [60], [64], [66], transition matrix approaches [24] and stochastic approaches [3], [55]. However, recent theoretical approaches for crowd dynamics can be typically distinguished in *macroscopic* models (refer, for instance, to [6], [16], [17], [28], [36], [37], [38], [42]), *mesoscopic/kinetics* methods (see [7], [8], [9], [10]) and *microscopic* models.

In particular, microscopic approaches (also called individual-based models, IBMs) describe a crowd as a collection of isolated pedestrians: each of them is individually considered, assimilated to a point particle or a quasi-rigid disk and followed during motion. More specifically, a first subgroup of microscopic models is represented by the so-called *cellular automata* (CA, see for instance [12], [43]), where each pedestrian behaves and moves according to a set of phenomenological rules that he/she executes depending on his/her individuality and/or as a reaction to extrapersonal stimuli (i.e., exerted by other walkers or by the surrounding environment). Another subtype of microscopic approaches includes instead the *discrete models*: they employ classical Newtonian laws of point mechanics, as the motion of each individual is described by an ordinary differential equation (ODEs). Several examples can be found in [30], [31], [32], [33], [54] and references therein.

Despite specific differences, most of microscopic-discrete models dealing with crowd dynamics show some significant similarities in the assumptions set up to establish pedestrian movement. First, walkers typically move according to a desired direction (i.e., the trajectory that minimizes the distance to their target destination) at a comfort velocity. Apart from complicated strategies, perturbations are typically assumed to result from two kinds of extrapersonal interactions: *social* and *physical*. The so-called social interactions do not have a physical source and reflect the desire of a pedestrian both to maintain a sufficient distance from other walkers and walls and/or to closely follow his/her groupmates, as in [34], [57]. On the other hand, physical interactions arise from collisions between individuals, or between an individual and a structural element within the domain. Both types of extrapersonal determinants are typically taken into account by a superposition of forces/velocity components (according to the order of the model).

However, unlike CA models, most purely discrete approaches pay little attention to the role played in crowd dynamics by the evolution of a pedestrian *environmental awareness*. As a matter of fact, the target destination (and therefore the relative direction of motion) of each individual is in fact typically established *a priori*, i.e., each pedestrian walks towards an initially-assigned destination. This is a serious shortcoming of microscopic-discrete models, since in reality a person may change his/her target destination according to new information learned about/from the surrounding environment, thereby giving rise to completely different dynamics of the whole crowd. For instance, when

moving within a building, an individual may dynamically change exit strategy: for example, he/she may opt for the nearest door, even if it is not the one he/she initially knew or decided to use. A walker is typically influenced by sounds or signage as well. In principle, a dynamic environmental awareness has to be coupled with a realistic evolution of the pedestrian gazing direction, which can be partially uncorrelated and independent from the pedestrian direction of movement. However, also this point has been disregarded by most discrete approaches presented in the literature so far.

The aim of the present work is indeed to describe a mathematical modeling environment able to address the above-mentioned critical issues. In particular, we propose a microscopic-discrete approach, where each pedestrian is characterized by his/her own preferred direction of movement, vision field and evolving environmental awareness. The combination of these ingredients represents a substantial improvement with respect to similar models present in the literature, as it allows to more realistically account for pedestrian decision-based behavior. Our mathematical environment is then tested with simulations dealing with crowd dynamics within two-dimensional built environments provided with several structural elements, such as corridors, dividers/columns, and exits.

The rest of this paper is organized as follows. In Section 2, we clarify the assumptions which our mathematical approach is based on and present the model components. More specifically, this first part does not still include a pedestrian dynamical environmental awareness (and the corresponding decision-based dynamics): this choice has been made to validate and compare our model against the pertinent computational literature. The resulting simulations, shown in Section 3, are able to capture selected experimentally-observed crowd patterns (i.e., streamline), and give interesting suggestions for designing corridor structures for smooth evacuations (i.e., in no strictly panic conditions). Then, in Section 4, we introduce the possibility for pedestrians to change target destination, as a consequence of new information acquired from the surrounding environment. In this sense, numerical realizations presented in Section 5 provide a clear confirmation of the role played by such a model development in reproducing more realistic dynamics. A discussion on results obtained by our approach, as well as on possible model improvements, is proposed in Section 6. The paper is finally equipped with an Appendix dealing with a sensitivity analysis of the main model parameters: in particular, it is focused on a justification of the parameter estimates and on their impact in the overall model behavior.

## 2 Mathematical model

### 2.1 Individual characteristics of single pedestrians

A crowd of  $N$  pedestrians is modeled in a domain  $\Omega \subseteq \mathbb{R}^2$ , which may reproduce the planimetry of a building. Within the domain, selected points of

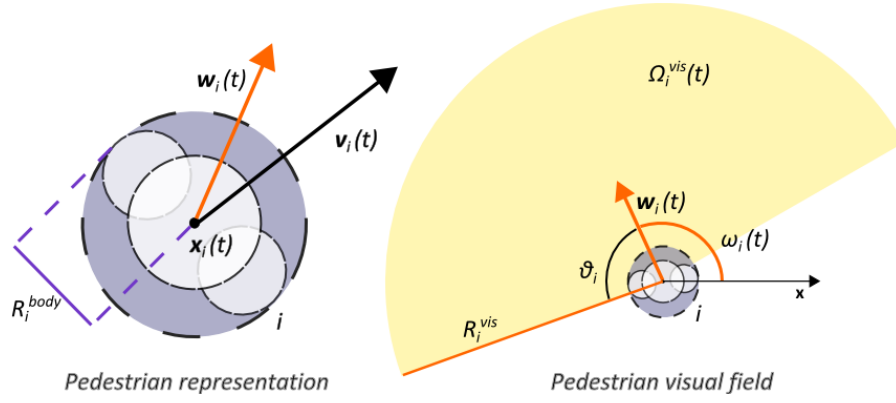


Fig. 1: Pedestrian characterization. Left panel: any pedestrian  $i$  is represented as a dimensionless point whose physical body is modelled as a circle of radius  $R_i^{\text{body}}$ .  $\mathbf{v}_i$  and  $\mathbf{w}_i$  indicate pedestrian's instantaneous velocity and gazing direction, respectively. Right panel: the pedestrian's gazing direction  $\mathbf{w}_i$  is defined by the angle  $\omega_i$  that it forms with the  $x$ -axis of the domain.  $\mathbf{w}_i$  indeed identifies the pedestrian's visual region  $\Omega_i^{\text{vis}}$ , where  $R_i^{\text{vis}}$  and  $\theta_i$  are the vision depth and the vision angle, respectively (refer to Eq. (3)).

interest for the considered walkers, such as exit doors, are identified. Each pedestrian  $i = 1, \dots, N$  is individually represented as a dimensionless point, whose position is identified by the vector  $\mathbf{x}_i$ . The physical space occupied by a walker is taken into account by defining a sphere of radius  $R_i^{\text{body}}$ , which corresponds to the major semiaxis of the ellipsoid obtained by overlapping three circles representing his/her head and shoulders (see Fig. 1, left panel). Each pedestrian is further characterized by a set of variables that completely describes his/her state

$$(s_i(t), \mathbf{v}_i(t), \mathbf{w}_i(t)). \quad (1)$$

$s_i$  is an integer number which defines the psychological condition of each pedestrian, i.e., his/her desire to maintain a given stride:

$$s_i(t) = \begin{cases} 0, & \text{if } i \text{ is walking normally;} \\ 1, & \text{if } i \text{ is in a hurry;} \\ 2, & \text{if } i \text{ is running;} \\ \dots & \end{cases} \quad (2)$$

The value of  $s_i$  may change in time as a result of personal and extrapersonal stimuli. The vectors  $\mathbf{v}_i$  and  $\mathbf{w}_i$  indicate instead the instantaneous velocity and gazing direction of an individual  $i$ , respectively. It is useful to stress that  $\mathbf{v}_i$  and  $\mathbf{w}_i$  are allowed to not be aligned and that can in principle vary independently.

In this respect, the gazing direction is a further pedestrian degree of freedom that, as we will see in the following, has an own evolution law. In particular,  $\mathbf{w}_i$  is determined by  $\omega_i$ , which is the angle between  $\mathbf{w}_i$  and the  $x$ -axis of the domain, i.e.,  $\mathbf{w}_i(t) = (\cos \omega_i(t), \sin \omega_i(t))$ , see the right panel of Fig. 1. The angle of vision of pedestrian  $i$  is set equal to  $\theta_i \in [0, \pi/2]$  both on the left and on the right of the gazing direction, so that his/her *visual region* finally reads:

$$\Omega_i^{\text{vis}}(t) = \left\{ \mathbf{y} \in S^2(\mathbf{x}_i(t), R_i^{\text{vis}}) : \frac{(\mathbf{y} - \mathbf{x}_i(t))}{|\mathbf{y} - \mathbf{x}_i(t)|} \cdot \mathbf{w}_i(t) \geq \cos(\theta_i) \right\}, \quad (3)$$

where  $S^2$  is the 2D-ball centered  $\mathbf{x}_i(t)$  with radius  $R_i^{\text{vis}}$ , which is the vision depth of the individual. The presence of structural obstacles (such as walls) obviously reduces pedestrian's visual region.

## 2.2 Pedestrian dynamics

To approach the dynamics of a generic pedestrian  $i$ , we start from a general second-order particle model:

$$m_i \frac{d^2 \mathbf{x}_i}{dt^2}(t) + \lambda_i \frac{d \mathbf{x}_i}{dt}(t) = \mathbf{F}_i(t), \quad (4)$$

where the constants  $m_i$  and  $\lambda_i$  are the mass and the friction coefficient, respectively, while  $\mathbf{F}_i$  denotes the sum of forces influencing walker behavior. However, living entities, such as cells, human crowds or swarms, are not passively prone to the Newtonian laws of inertia, as they are able to actively develop behavioral strategies which depend both on intrinsic stimuli and on the interaction with the external environment. For instance, a pedestrian, at least when he/she is not running too quick, can decide to stop and change direction of motion: intelligence can be in fact regarded also as the ability of an individual to actively control his/her body and therefore his/her movement, see also [19]. These concepts allow to neglect the inertial term in Eq. (4), i.e., to assume, in mathematical terms,  $\lambda_i \gg m_i$ :

$$\underbrace{\frac{m_i}{\lambda_i} \frac{d^2 \mathbf{x}_i}{dt^2}(t)}_{\rightarrow 0} + \frac{d \mathbf{x}_i}{dt}(t) = \frac{\mathbf{F}_i(t)}{\lambda_i} \Rightarrow \frac{d \mathbf{x}_i}{dt}(t) = \frac{\mathbf{F}_i(t)}{\lambda_i} = \underbrace{\tilde{\mathbf{v}}_i(t)}_{\text{pedestrian velocity}}. \quad (5)$$

Eq. (5) states that the velocity of an individual, and not his/her acceleration, is proportional to the acting forces. This relation, called *overdamped force-velocity response*, is at the basis of a number of discrete/IBM approaches (see [23] and [62] for comments) and allows to describe selected pedestrian behavior by a direct phenomenological postulation of the velocity contributions, i.e., by a first-order model. The actual speed of a walker is finally established by his/her desire and subjected to physical constraints.

Taking into account of all the above-explained considerations, the equation of motion of a pedestrian  $i$  reads as

$$\frac{d\mathbf{x}_i}{dt}(t) = \tilde{\mathbf{v}}_i(t) = \min\{\bar{v}(s_i(t)), |\mathbf{v}_i(t)|\} \frac{\mathbf{v}_i(t)}{|\mathbf{v}_i(t)|}. \quad (6)$$

In Eq. ((6)),  $\bar{v}(s_i(t))$  defines the comfort speed of the individual, established according to his/her personal status  $s_i$  (see Eq. (2)):

$$\bar{v}(s_i(t)) = \begin{cases} \bar{v}_0, & \text{if } s_i(t) = 0; \\ \bar{v}_1, & \text{if } s_i(t) = 1; \\ \bar{v}_2, & \text{if } s_i(t) = 2; \\ \dots & \end{cases} \quad (7)$$

In particular,  $\bar{v}_0 < \bar{v}_1 < \bar{v}_2 < \dots \leq \bar{v}_{\max}$ , where  $\bar{v}_{\max}$  is a maximal value coherent with human physical limitation (i.e., a maximal acceptable speed). An analogous thresholding over the individual velocity has been earlier proposed in the celebrated Helbing's model (see [27]) and used to avoid unrealistically high speeds, that might arise even from realistic dynamics.

We then assume that the dynamics of each pedestrian derive from the combination of both *social/behavioral* and *physical* forces. The so-called social forces (a concept introduced by Helbing and co-workers in the 90's, see [27], [31], [32], [34], [57]) do not have a physical source, but rather reflect the intentions of a pedestrian to reach some target destinations (e.g., exits) at a given speed and to keep a certain distance from walls and from strangers. Moreover, when collisions between pedestrians happen, physical forces of pushing and friction enter the picture. In other words, we can say that the instantaneous movement of a pedestrian is the result of his/her own strategy (developed by taking into account his/her purpose) and of the interactions with the surrounding environment and the walkers encountered along his/her motion. Then, the velocity components of the generic pedestrian  $i$  read as follows:

$$\mathbf{v}_i(t) = \underbrace{\mathbf{v}_i^{\text{des}}(t)}_{\substack{\text{individual strategy} \\ \text{env. influence}}} + \underbrace{\mathbf{v}_i^{\text{crowd}}(t)}_{\substack{\text{interpersonal} \\ \text{interactions}}} + \underbrace{\xi_i(t)}_{\text{noise}}, \quad (8)$$

where  $\mathbf{v}_i^{\text{des}}$  is the individual strategy and  $\mathbf{v}_i^{\text{crowd}}$  represents the velocity contributions due to interactions with surrounding walkers. Finally,  $\xi_i$  is a fluctuation term, that deals with variations of pedestrian behavior from the given rules of motion. In this respect, the fluctuation term may account for accidental events, as commented in similar models [27], or may model the uncertainty of individual reactions to the same stimuli. From a mathematical point of view,  $\xi_i$  can be in principle described by a vector whose modulus is  $\bar{v}(s_i(t))$  and whose direction is established by a given probabilistic distribution (for example, a gaussian law).



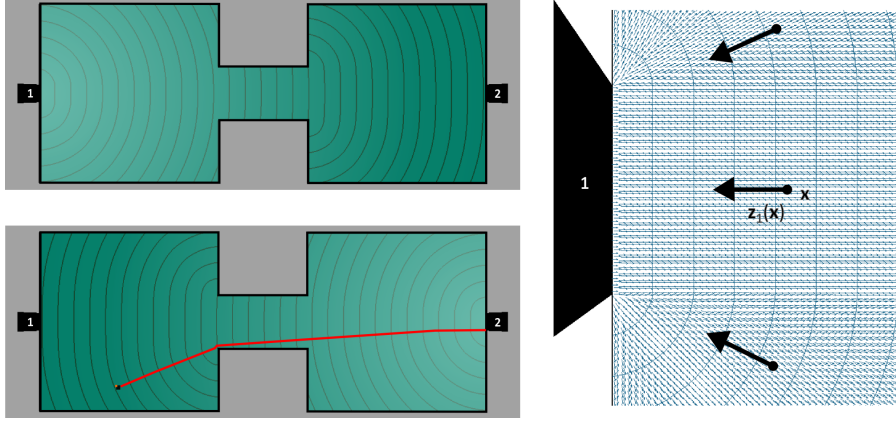


Fig. 2: A representative domain reproducing the planimetry of a building composed of two rooms. Each room is equipped with an exit door, that constitutes a possible pedestrian target destination. Left panel, top: signed distance function for the exit door in the left room (color field, lighter colors indicate shorter arrival times). Left panel, bottom: signed distance function for the exit door in the right room (color field, lighter colors indicate shorter arrival times), isochronal loci for different values of the arrival time (black contours), trajectory followed by a single pedestrian to reach the exit door in the right room (red thick line). Right panel: magnification of the gradient field of the signed distance function.

### 2.2.1 Personal desired strategy.

The first term in Eq. (8) describes the attempt of a generic pedestrian  $i$  to move in his/her preferred direction at his/her comfort velocity. Such a personal component of the velocity is assumed to depend on the position of the target destination and on the natural intention to stay sufficiently away from walls. Indeed, we have:

$$\mathbf{v}_i^{\text{des}}(t) = \mathbf{v}_i^{\text{targ}}(t) + \mathbf{v}_i^{\text{wall}}(t). \quad (9)$$

*Target velocity.* The target velocity of each pedestrian is established according to his/her desire to minimize the effort to reach his/her target destination, i.e., to cover the shortest possible path from his/her position to his/her target destination at his/her preferred speed (other strategic behavior may be taken into account).

Indeed, let us label each possible point of interest for pedestrians with an integer number  $h = 1, \dots, H$ , so that the target destination of the  $i$ -th individual can be indicated by  $h_i \in \{h\}_1^H$ . A target destination can be any point within the domain, any subset of domain's boundaries (e.g., an exit door), or any subset of the domain (e.g., a target area where a pedestrian needs to gather).

The target velocity of pedestrian  $i$  is given by:

$$\mathbf{v}_i^{\text{targ}}(t) = \bar{v}(s_i(t)) \mathbf{z}_{h_i}(\mathbf{x}_i(t)) \quad (10)$$

where  $\bar{v}$  is his/her comfort speed value, as specified in Eq. (7). The unit vector  $\mathbf{z}_{h_i}(\mathbf{x}_i(t))$  represents the local tangent vector to the trajectory joining the instantaneous position of the  $i$ -th pedestrian to his/her target destination with the shortest arrival time (in short, *optimal trajectory*).

Computation of optimal trajectories is a well-consolidated subject; so, in principle, the optimal path for a given pedestrian with a given target destination can be computed by using any of the available methods in the existing literature. For instance, in polygonal domains, the trajectory to a target destination with the shortest arrival time is a piece-wise linear curve, which can be computed using the visibility graph (see for instance, [1]). Other approaches can be considered in case of non-polygonal or non-planar domains (where the optimal trajectory must be replaced with the optimal geodesic path), but at the price of increasing the computational cost.

If we neglect interpersonal collisions, each pedestrian would follow the optimal trajectory to his/her target destination without any deviation. Therefore, the optimal trajectory could be computed for each pedestrian once and for all after assigning his/her destination. In our model, however, each walker can change his/her target destination due to new information acquired from the surrounding environment, and can also deviate from the optimal trajectory due to inter-personal collisions. For these reasons, the optimal trajectory must be recomputed at each time step for each pedestrian according to his/her instantaneous position and his/her target destination, thus leading to an unacceptable computational cost.

In order to avoid to continuously recompute the optimal trajectory, we adopt the following strategy. For each target location  $h = 1, \dots, H$  (e.g., a door), we compute the distance function  $\Phi_h(\mathbf{x}) : R^2 \rightarrow R_+ \cup \{0\}$ , defined as follows:

$$\Phi_h(\mathbf{x}) := \min_{\mathbf{y} \in \bar{\Gamma}_h} d(\mathbf{x}, \mathbf{y}), \quad \forall \mathbf{x} \in \Omega \quad (11)$$

where  $\bar{\Gamma}_h$  is the closure of the subdomain  $\Gamma_h$  that forms the location of interest  $h$  and  $d(\mathbf{x}, \mathbf{y})$  is the usual Euclidean distance. It can be proved that the signed distance function  $\Phi_h$  is the solution to the 2D Eikonal equation:

$$|\nabla \Phi_h(\mathbf{x})|^2 = 1 \quad (12)$$

with condition:

$$\Phi_h(\mathbf{x}) = 0, \quad \mathbf{x} \in \bar{\Gamma}_h. \quad (13)$$

Note that the above problem is well-posed even if boundary conditions are not supplied on  $\partial\Omega \setminus (\partial\Omega \cap \bar{\Gamma}_h)$ . In fact, a simple analysis of the 2D Eikonal equation shows that characteristics emanate from  $\bar{\Gamma}_h$  and cross domain boundaries from domain's interior both in case of a target destination located inside the domain, and in case of a target destination located on its boundaries.

It follows from Eq. (11), that the local unit tangent vector to the optimal trajectory from the location of pedestrian  $i$  to his/her target destination  $h_i$  is simply given by:

$$\mathbf{z}_{h_i}(\mathbf{x}_i) = -\nabla\Phi_{h_i}(\mathbf{x}_i). \quad (14)$$

The above strategy has three major advantages. First, the problem in Eqs. (12)-(13) can be solved only once for each target location. This can be accomplished very efficiently using, for instance, the fast-marching technique introduced in [45] and [46]. Second,  $\mathbf{z}_{h_i}$  can be evaluated without explicitly computing the optimal trajectory for each pedestrian at each time step, thus avoiding a significant computational effort. Third, algorithm complexity is independent of domain geometry and can be easily generalized also to the case of non-planar domain. An example of signed distance function is depicted in Fig. 2.

Recent alternative approaches for evaluating pedestrian optimal paths may also include minimum time length algorithms (see [51] and references therein).

*Wall repulsion velocity.* The desired shortest path, mainly in complex domains, could be unrealistically close, or even superposed, to walls or non-walkable structures such as columns. However, the intention of individuals to stay sufficiently away from such architectural elements can be implemented by introducing a repulsive term for any pedestrian  $i$ , that is active only when he/she is close enough to one of them:

$$\mathbf{v}_i^{\text{wall}}(t) = \begin{cases} -A_i \exp\left((R_i^{\text{body}} - d_i^{\text{wall}}(\mathbf{x}_i(t)))/B_i\right) \mathbf{n}_i^{\text{wall}}(\mathbf{x}_i(t)), & \text{if } d_i^{\text{wall}}(\mathbf{x}_i(t)) \leq R_i^{\text{wall}}, \\ 0, & \text{else,} \end{cases} \quad (15)$$

where  $A_i$  and  $B_i$  are constants and

$$\mathbf{n}_i^{\text{wall}}(\mathbf{x}_i(t)) = \frac{\nabla d_i^{\text{wall}}(\mathbf{x}_i(t))}{|\nabla d_i^{\text{wall}}(\mathbf{x}_i(t))|}$$

is the unit vector directed from the position of individual  $i$  toward the nearest point of the non-walkable element, as  $d_i^{\text{wall}}(\mathbf{x}_i(t))$  is corresponding distance, as done for instance in [29], [57]. Finally,  $R_i^{\text{wall}} > R_i^{\text{body}}$  is the *wall repulsion radius*.

### 2.2.2 Interpersonal interaction velocity

The interaction component of the velocity of pedestrian  $i$  is the sum of different contributions, which implement both physical/contact and social/repulsive forces:

$$\mathbf{v}_i^{\text{crowd}}(t) = \mathbf{v}_i^{\text{cont}}(t) + \mathbf{v}_i^{\text{rep}}(t). \quad (16)$$

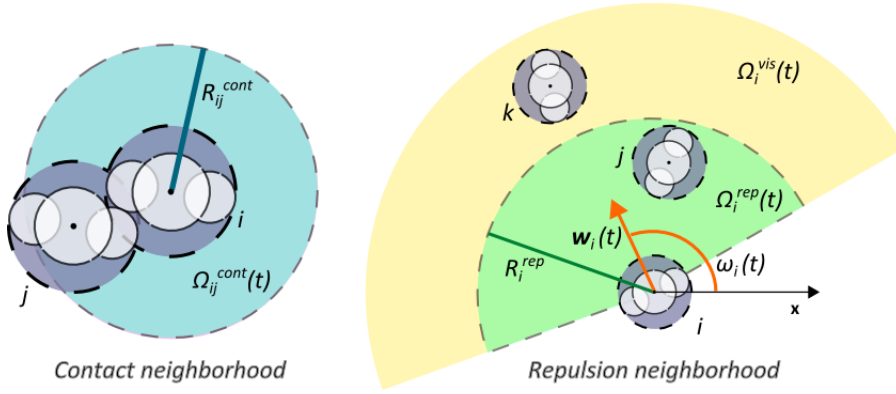


Fig. 3: Pedestrian interaction neighborhoods. Left panel: the contact neighborhood  $\Omega_{ij}^{cont}$  ensures that a pair of walkers  $i, j$  collides when their relative distance is lower than the sum of their body radius, as  $R_{ij}^{cont} = R_i^{body} + R_j^{body}$ . Right panel: the contact neighborhood  $\Omega_i^{cont}$  models the desire of pedestrian  $i$  to keep distance from the walkers within his/her visual region  $\Omega_i^{vis}$ .

*Contact velocity.* The contact component of the interaction velocity describes the physical forces of pushing and sliding friction between two colliding pedestrians. It is a purely physical force that accounts for the mass of each walker. In particular, the contact velocity term of an individual  $i$  is given by the superposition of binary interactions, as

$$\begin{aligned}
 \mathbf{v}_i^{cont}(t) &= \sum_{\substack{j=1 \\ \mathbf{x}_j(t) \in \Omega_{ij}^{cont}(t)}}^N \mathbf{v}_{ij}^{cont}(t) = \\
 &= \sum_{\substack{j=1 \\ \mathbf{x}_j(t) \in \Omega_{ij}^{cont}(t)}}^N \left[ \underbrace{-C_i(R_{ij}^{cont} - |\mathbf{x}_j(t) - \mathbf{x}_i(t)|) \mathbf{n}_{ij}(\mathbf{x}_j(t), \mathbf{x}_i(t))}_{\text{body force velocity}} \right] \\
 &+ \sum_{\substack{j=1 \\ \mathbf{x}_j(t) \in \Omega_{ij}^{cont}(t)}}^N \left[ \underbrace{D_i(R_{ij}^{cont} - |\mathbf{x}_j(t) - \mathbf{x}_i(t)|) \mathbf{t}_{ij}(\mathbf{x}_j(t), \mathbf{x}_i(t))}_{\text{sliding friction velocity}} \right].
 \end{aligned} \tag{17}$$

The *contact neighborhood* of pedestrian  $i$  is

$$\Omega_{ij}^{cont}(t) = \{\mathbf{y} \in \Omega : |\mathbf{y} - \mathbf{x}_i(t)| \leq R_{ij}^{cont}\}, \tag{18}$$

so that the corresponding component of his/her velocity comes into play only when he/she gets close enough to another pedestrian  $j$ , so that both experience a physical collision (see Fig. 3). The contact radius  $R_{ij}^{cont} = R_i^{body} + R_j^{body}$  is the sum of the body radii of colliding pedestrians, while  $|\mathbf{x}_j(t) - \mathbf{x}_i(t)|$  is their

distance. The unit vectors  $\mathbf{n}_{ij}$  and  $\mathbf{t}_{ij}$  are respectively defined as

$$\mathbf{n}_{ij}(\mathbf{x}_j(t), \mathbf{x}_i(t)) = \frac{\mathbf{x}_j(t) - \mathbf{x}_i(t)}{|\mathbf{x}_j(t) - \mathbf{x}_i(t)|}, \quad (19)$$

$$\mathbf{t}_{ij}(\mathbf{x}_j(t), \mathbf{x}_i(t)) = \mathbf{k} \times \mathbf{n}_{ij}(\mathbf{x}_j(t), \mathbf{x}_i(t)),$$

where  $\mathbf{k}$  is the unit vector perpendicular to the plane of motion. Finally,  $C_i$  and  $D_i$  are constant parameters, whose value will be estimated in the Appendix and listed in Table 1. It is useful to notice that we are assuming *isotropic* contact interactions, as one can collide also with individuals coming from behind. In mathematical terms, for any pair  $i, j$  of walkers, if  $\mathbf{x}_j(t) \in \Omega_{ij}^{\text{cont}}(t)$  at a given time  $t$ , then  $\mathbf{x}_i(t) \in \Omega_{ji}^{\text{cont}}(t)$ . The contact terms introduced in (17) represent a slightly modification of the corresponding acceleration corrections employed in [34].

*Repulsion velocity.* The repulsive term is introduced to reproduce the natural tendency of pedestrians (at least in non-panic situations) to keep a distance from surrounding individuals (the so-called *territorial effect*) and to avoid collisions in cases of sudden velocity changes. Then, assuming again binary repulsive interactions, we have:

$$\begin{aligned} \mathbf{v}_i^{\text{rep}}(t) &= \sum_{\substack{j=1 \\ \mathbf{x}_j(t) \in \Omega_i^{\text{rep}}(t)}}^N \mathbf{v}_{ij}^{\text{rep}}(t) \\ &= \sum_{\substack{j=1 \\ \mathbf{x}_j(t) \in \Omega_i^{\text{rep}}(t)}}^N -E_i \exp((R_{ij}^{\text{cont}} - |\mathbf{x}_j(t) - \mathbf{x}_i(t)|)/F_i) \mathbf{n}_{ij}(\mathbf{x}_j(t), \mathbf{x}_i(t)), \end{aligned} \quad (20)$$

where  $E_i$  and  $F_i$  are constant coefficients (again estimated in the Appendix and listed in Table 1), and  $R_{ij}^{\text{cont}}$  and  $\mathbf{n}_{ij}(\mathbf{x}_j(t), \mathbf{x}_i(t))$  are defined as in Eq. (17).  $\Omega_i^{\text{rep}}$  represents instead the *repulsion neighborhood* at a given time  $t$  of a generic pedestrian  $i$ , determined by the compact

$$\Omega_i^{\text{rep}}(t) = \{\mathbf{y} \in \Omega_i^{\text{vis}}(t) \cap \Omega : |\mathbf{y} - \mathbf{x}_i(t)| \leq R_i^{\text{rep}}\}, \quad (21)$$

where the visual region  $\Omega_i^{\text{vis}}$  reads as in (3) and the repulsion radius  $R_i^{\text{rep}}$  represents the radius of his/her private sphere, i.e., the extension of the surrounding space he/she intends to preserve. It is worthy to stress that, unlikely the case of contact interactions, the repulsive velocity corrections are *anisotropic*, as they are only active within the pedestrian vision field. This is consistent with the fact that walkers rarely react to situations happening behind them. Indeed, if a pedestrian  $j$  falls in the repulsion neighborhood of  $i$ , i.e.,  $\mathbf{x}_j(t) \in \Omega_i^{\text{rep}}(t)$  at a certain time  $t$ , it is not necessarily true that  $\mathbf{x}_i(t) \in \Omega_j^{\text{rep}}(t)$  at the same time  $t$ . The anisotropy of the interpersonal repulsion term is not entirely new in the literature, but it is widely related to the individual direction of motion. In fact, it is usually assumed that pedestrians desire more open space in their

walking direction than in others [29], [32]. Such an hypothesis is reasonable in a first approximation: however, we strongly believe that a more realistic repulsion neighborhood has to be related with the individual gazing direction, as a pedestrian *must see* other walkers in order to avoid them.

### 2.3 Evolution of the gazing direction

During motion, each pedestrian may turn his/her gazing direction i) to reduce the head rotation w.r.t. his/her movement direction, ii) to acquire new information from the surrounding environment (i.e., to include a specific point in his/her vision region), iii) for some unconscious fluctuations (noise). In more details, recalling the relation between the gazing direction of individual  $i$  and the angle  $\omega_i$  defined in Section 2.1, the temporal evolution of  $\mathbf{w}_i(t)$  is determined by the following equation:

$$\frac{d\omega_i}{dt}(t) = - \underbrace{G_i (\mathbf{v}_i(t) \times \mathbf{w}_i(t)) \cdot \mathbf{k}}_{\text{head rotation}} - \underbrace{\sum_m P_{im} (\mathbf{p}_m(t) \times \mathbf{w}_i(t)) \cdot \mathbf{k}}_{\text{external stimuli}} + \underbrace{\zeta_i(t)}_{\text{noise}}, \quad (22)$$

where  $G_i$  and  $P_{im}$  are constant coefficients,  $\mathbf{k}$  is as usual the unit vector perpendicular to the plane of motion, and  $\mathbf{p}_m$  indicates the location of the external stimulus  $m$  that can capture pedestrian attention. Finally,  $\zeta_i$  is a random fluctuation term for the evolution of the pedestrian gazing direction. It may describe unpredictable individual reactions to environmental stimuli or accidental head rotations. For these reasons, possible modeling laws for  $\zeta_i$  may be (i) a uniform distribution over the range of values  $[\omega_i - \theta_i; \omega_i + \theta_i]$  or (ii) a gaussian distribution with mean  $\omega_i$  and standard deviation  $\theta_i/2.58$ , i.e., in order to have the 99% of probability that  $\zeta_i$  belongs to the individual visual field.

For the reader's convenience, we stress that the first term in Eq. (22) employs the head rotation of a pedestrian in the direction of his/her motion: it is therefore conceptually the opposite of the velocity correction used in [57], that instead assumes that pedestrians adjust their position to reduce the head rotation. Such a difference of viewpoints is due to the fact that, in [57], pedestrians want to maintain their groupmates within their visual field. Indeed, once their gazing direction has been established by the position of the other individuals, they have to necessarily move accordingly.

## 3 Numerical results - I

### 3.1 Simulation details

In the next sections, we show numerical results in two-dimensional domains  $\Omega \subset \mathbb{R}^2$ , which reproduce the planimetry of buildings characterized by the presence of rooms, exit doors, corridors, columns and internal/external walls.

Table 1: Summary of the parameters used in the model.

Parameter	Description	Value	Units
$R^{\text{body}}$	pedestrian body radius	0.3	m
$R^{\text{vis}}$	pedestrian visual depth	50.0	m
$\theta$	pedestrian visual angle	1.48	rad
$\bar{v}_0$	desired speed of calm pedestrians	1.33	$\text{m s}^{-1}$
$A$	wall repulsion coefficient	1.0	$\text{m s}^{-1}$
$B$	wall repulsion coefficient	0.01	m
$R^{\text{wall}}$	wall repulsion radius	0.4	m
$C$	contact force coefficient	25.0	$\text{s}^{-1}$
$D$	contact force coefficient	50.0	$\text{s}^{-1}$
$E$	interpersonal repulsion coefficient	1.0	$\text{m s}^{-1}$
$F$	interpersonal repulsion coefficient	0.5	m
$R^{\text{rep}}$	interpersonal repulsion radius	3.0 / 1.0	m
$G$	gazing direction coefficient	2.0	$\text{rad s m}^{-1}$

In all simulations, the entire crowd of pedestrians is characterized by the very same physical determinants and social behavior, except from initial target destinations that, as it will be specified, can depend on the specific walker (or walker subgroup). It is worthy to stress that, in principle, it would have been possible to differentiate the characteristics of each single pedestrian, as the relative parameters are individually defined. In particular, the parameters of our model can be divided in (i) directly interpretable and measurable quantities, like the interaction radii and the dimensions of the visual region, and (ii) technical coefficients, that determine the impact of each velocity component but that do not have an immediate physical correspondence (i.e.,  $A_i, B_i, C_i, D_i, E_i, F_i, G_i$ ). In both cases, we here list their value, providing a short comment on how they have been estimated and, when possible, a proper reference to the literature of the field. However, we remaind the reader to the Appendix of this paper for a detailed sensitivity analysis, that justifies the choices made for the parameter setting and studies the relative impact on the simulation outcomes.

All pedestrians have a body radius  $R_i^{\text{body}} = R^{\text{body}}$  which is estimated equal to 0.3 m (i.e., they are assumed to be adult medium-sized individuals, as commonly done in similar models, see [63] and [67]). The walkers' visual region  $\Omega_i^{\text{vis}}$ , defined in Eq. (3), is instead defined by a visual depth  $R_i^{\text{vis}} = R^{\text{vis}} = 50$  m and by a visual angle  $\theta_i = \theta = 1.48$  rad (i.e.,  $\approx 85^\circ$ ), see the considerations in [11]. In all the following sets of simulations, we further assume that all pedestrians are calm during the entire dynamics, i.e., no events take place which can perturb their status: hence,  $s_i(t) = 0$  for any  $i$  and any  $t$ . From this hypothesis, it follows an common comfort speed  $\bar{v}_0 = 1.33 \text{ m s}^{-1}$ , which is a realistic value for individuals in a no-hurry status, (as commented in the already cited published work [67]). The wall repulsion force acts on any pedestrian  $i$  when his/her distance from walls is lower then  $R_i^{\text{wall}} = R^{\text{wall}} = 0.4$  m, while the constants  $A_i = A$  and  $B_i = B$  in Eq. (15) are estimated equal to  $1 \text{ m s}^{-1}$  and  $0.01 \text{ m}$ , respectively. Both contact and repulsion forces are

independent from the specific pair of interacting individuals: particularly, given  $R_{ij}^{\text{cont}} = R_i^{\text{body}} + R_j^{\text{body}} = 2R^{\text{body}} = 0.6$  m, we set, for any  $i$ , the contact constants  $C_i = C$  and  $D_i = D$  equal to  $25 \text{ s}^{-1}$  and  $50 \text{ s}^{-1}$ , respectively. Then, the common repulsion radius is estimated in a realistic fashion  $R_i^{\text{rep}} = R^{\text{rep}} = 3$  m. However, in the sets of simulations dealing with evacuation issues (cf. Section 3.3),  $R^{\text{rep}}$  is reduced to 1 m: this is consistent, since individuals trying to get out as soon as possible from a building care less of the territorial effect. Instead, the repulsion constants  $E_i = E$  and  $F_i = F$  are always set equal to  $1 \text{ m s}^{-1}$  and  $0.5$  m, respectively. We also assume the absence of any external stimuli that can induce pedestrians to suddenly turn their gaze (i.e., the second term at the r.h.s. of (22) is neglected). In the same equation, we set  $G_i = G = 2$  (rad s)  $\text{m}^{-1}$  for any  $i$ . In all realizations, we finally assume that the evolution both of pedestrian velocity and of gazing direction are not affected by fluctuation terms, i.e.,  $\xi(t)_i = \zeta_i(t) \equiv 0$  for any  $t$  and  $i$ , as it is done in the well-known Helbing's social force model [27].

In all the simulations proposed in the next sections, the domain boundary  $\partial\Omega$  is formed either by walls or by exit doors. The exit doors represent possible pedestrian points of interest  $h$ : in this respect, if a walker falls within (or cross) a part of the domain border occupied by a door, say  $\bar{T}_h \subset \partial\Omega$  (recalling the same notation as in Section 2.2.1), he/she is assumed to have reached his/her target and he/she is therefore eliminated from the system. On the opposite, an individual is obviously not allowed to trespass external/internal walls and other structural elements, such as columns. This critical situation is not *a priori* avoided by the introduction of the threshold on the velocity and of a proper wall repulsion law, but it is here computationally prevented with a *predictor-corrector* scheme. Entering in more details, the position of each pedestrian is firstly estimated using the entire simulation time step (predictor). If a walker results to cross a domain boundary (that may happen if the integration time step is over-estimated), the following procedure is activated: (i) the exact time at which “the collision” with the wall occurs is computed by backwards integration along the trajectory and (ii) from such an exact time, until the end of the actual time step, the pedestrian is set to move along the wall (corrector).

### 3.2 Streamline formation

We first deal with two rooms of  $20 \times 20 \text{ m}^2$ , connected by a corridor 10 m long and 6 m wide. A crowd of 100 pedestrians is equally divided in two groups, each located in a room. The target destination of the pedestrians initially located in the left room (black points in Fig. 4) is the exit door in the right room, while the target destination of the pedestrians initially located in the right room (white points in Fig. 4) is the exit door in the left room. This choice is done to obtain sufficiently long walker paths, which may result in interesting collective dynamics, mainly emerging in the hallway passage.



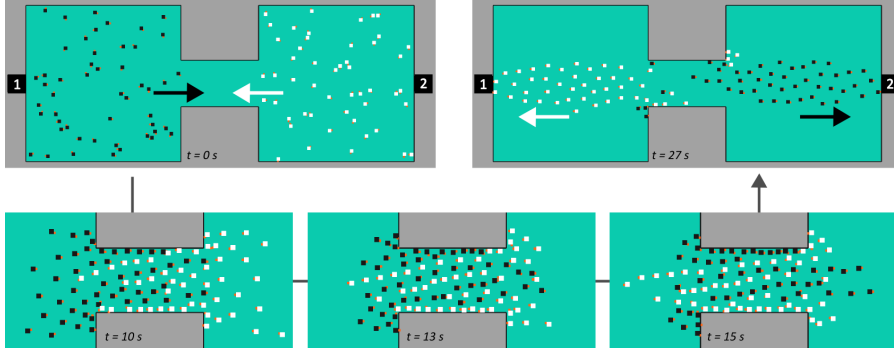


Fig. 4: Crowd dynamics in a building composed of two rooms and a 6 m-wide corridor. Several ordered counter-stream queues autonomously emerge when two groups of pedestrians walking in opposite directions encounter within the corridor. The orange dot near to each individual indicate his/her gazing direction, which is initially randomly generated. Representative images taken at  $t = 0, 10, 13, 15, 27$  seconds.

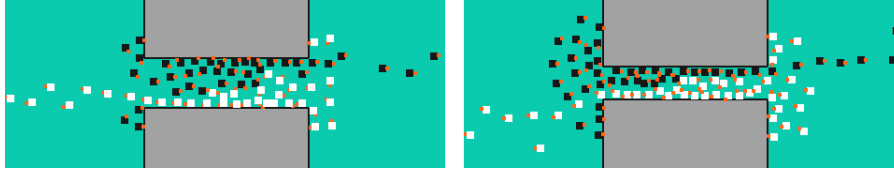


Fig. 5: Effect of the corridor width on the streamline formation. A progressive reduction in the corridor width (to 3 and 2 meters, left/right respectively) results in the subdivision of the passage in two larger lanes characterized by a uniform direction of motion.

At the initial stages of motion, until the two groups are well separated, each pedestrian moves according to his/her target destination and deviates his/her walking direction because of the presence of walls, and because of interactions with surrounding walkers (that, belonging to the same group, therefore have the same preferred direction of motion), see Fig. 4. Then, in order to reach the respective target doors, the two groups necessarily have to enter the corridor in opposite directions, thereby encountering and partially obstructing the passage each other. As a result, we observe the self-emergence of several, almost parallel, one-individual-wide counter-stream queues, each formed by pedestrians belonging to the same group, as reproduced in Fig. 4. Such collective dynamics are due to specific individual-scale behavior: the single walkers have in fact to perform little sideways adjustments to continue their motion towards their own target destinations. From an energetic point of view, it is in fact more efficient for them, in terms of deviation maneuvers, to follow the path of another groupmate than to create a new path in the crowded

hallmark structure. Finally, all pedestrians are able to reach their target exit door, even if they acquire again an uncorrelated disordered migration.

The formation of pedestrian streamlines, empirically observed in real-world scenarios involving bottleneck and narrow architectures [27], [41], [49], [50], has been captured and reproduced with different types of mathematical approaches. However, in the case of both macroscopic [18] and microscopic-discrete [34] models, the simulation outcomes are significantly affected by a long-range *attraction* term between individuals of the same group that biases walker movement enforcing groupmate aggregation. In this respect, it is useful to underline that we do not employ such a type of velocity contribution since, in our assumption, the subgroups of the overall crowd are composed of individuals who do not know each other (i.e., they are not “real” group-mates) but only share the same target destination. A self-emergent formation of walker streamlines can be instead more easily captured by rule-based cellular automata, see [2], [59] and references therein.

We next turn to analyze how changes in the planimetry of the build environment affect the model outcome. As reproduced in Fig. 5, a progressive reduction in the corridor width (to 3 and 2 meters, respectively) results in the formation of two lanes of pedestrians walking in opposite directions. Due to the decreased availability of free space in these cases, individuals are closely packed to each other and to surrounding walls. It is also interesting to notice how such lanes start as being composed of two (or even three) pedestrians in parallel to end up in single-individual-wide queues toward the end of the corridor. The rationale of these dynamics is that, in overcrowded narrow structures, the only way for groups of walkers to go on moving in opposite directions is no longer to create one-person-wide counter-stream queues but to autonomously subdivide the passage in two larger lanes characterized by a uniform direction of motion. In real-world scenarios, as tunnels, subway stations or bridges, such an emerging pattern is further encouraged and stabilized by structural elements, i.e., internal walls, columns or trees, as commented again in [34].

### 3.3 Optimization of a pedestrian facility for evacuation purposes

In this section, we perform numerical simulations specifically designed to present a preliminary study relative to the optimization of a pedestrian facility. More specifically, we focus on evacuation dynamics (in no panic conditions) of a crowd composed of 200 pedestrians from a room through different narrow passages. The effect of the specific planimetry is evaluated comparing the *evacuation time* in the different cases. The evacuation time is defined as the time needed by the entire crowd to enter the target “safe-room” (i.e., the other w.r.t. their initial location). For the reader’s convenience, we recall that in the following sets of realizations  $R^{\text{rep}}$  is reduced to 1 m.

In the first family of simulations, we consider the same planimetry introduced in the previous test case. Here, however, the width of the corridor between the two adjacent rooms has been varied for each realization and also

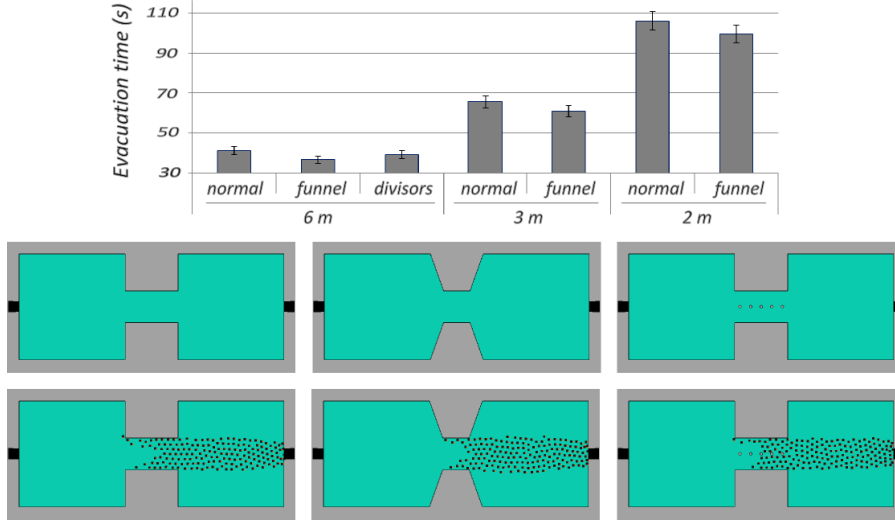


Fig. 6: Effect of the corridor shape and measures on the evacuation time of a crowd. We deal with 6, 3, and 2 m-wide corridors with or without a funnel-like entrance. We also study the role of a series of divisors placed in the middle of the widest corridor. In the bottom lines of panels, we represent the different types of architectural solutions tested and some representative images of the corresponding pedestrian dynamics. All the values in the plot are represented as means  $\pm$  SD over 50 realizations, characterized by the same parameter setting but different initial distributions of the same number of pedestrians.

funnel-shape constructions and obstacles in corridor have been added for the second and third serie of realizations, respectively (see Fig. 6). More in details, all pedestrians are initially distributed in the left room, while the door in the right room is their common target destination. As summarized in the plot of Fig. 6 (top panel), it is immediately evident that narrower corridors result in increments in the evacuation time. Moreover, it is possible to observe that, at any corridor width, funnel-like geometries facilitate pedestrian evacuation. This is due to the fact that a funnel-shape entrance of the corridor allows a gradual modulation of walker velocity and direction of motion, thereby reducing the formation of possible overcrowded obstructions (at the bottleneck). A further case of interest is the case with the widest corridor and a series of divisors distributed along the medial axis (see Fig. 6 (bottom right panel)). Such an architectural solution, however, has a little effect on the evacuation dynamics. This is probably a consequence of the fact that the corridor is large enough to allow a smooth flux of pedestrians. Moreover, since all walkers have the same target destination, there is no necessity of creating and stabilizing counter-stream lanes with structural elements.

We next employ our model on a planimetry representing two adjacent rooms, separated by an internal wall. In this case, the narrow passage is con-

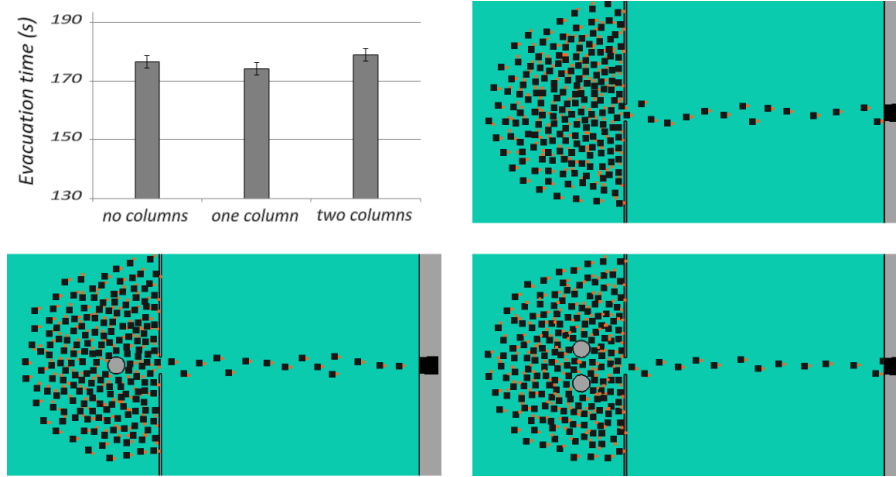


Fig. 7: Effect of the presence of columns on the evacuation time of a crowd, in the case of two adjacent rooms separated by an internal wall with a 1 m-wide door. The evacuation time does not significantly change as a consequence of the specific architectural solutions. However, the presence of columns reduces the clogging effect occurring near the exit door. All the values in the plots are represented as means  $\pm$  SD over 50 realizations, characterized by the same parameter setting by different initial distributions of the same number of pedestrians.

stituted by a 1 m-large door. Again, the group of individuals is initially placed in the left room and wants to evacuate through the exit door of the right room. As reproduced in Fig. 7, the absence or the presence of columns in front of the internal door does not significantly affect the evacuation time of the crowd (i.e., the difference in the corresponding evacuation times is less than 10 seconds). However, it is possible to observe that the addition of columns prevents dramatic clogging effects in the proximity of the exit door. Such structural elements force in fact a subdivision of walkers, thereby reducing the pressure within the crowd mass. As captured in the bottom panels of Fig. 7, the evacuating individuals are more spaced near the exit door, preserving a more extended “vital neighborhood”. These results agree with literature, where such types of structure modifications are typically tested in panic conditions, in order to preliminarily control and avoid critical situations especially in the case of mass events. More specifically, it is interesting to notice that the range of evacuation time in the case of adjacent rooms are comparable to those measured in a similar, although of second order, discrete model dealing with an analogous domain, see [34].

#### 4 Model extension: introduction of pedestrian environmental awareness

In a great number of situations, pedestrians may change target destination according to a dynamical synthesis between their initial purpose and the evolution of their environment awareness, which is improved by acquiring new information about surrounding environment during motion. For instance, a walker aiming to get out as soon as possible from a building is firstly induced to reach the exit he/she used to come into the building. However, during motion, he/she may discover a new exit door, that may be preferable from a strategic point of view. The improved environmental awareness allows the pedestrian to opt for a change of the target destination. In other words, the pedestrian motion is the result of a dynamical decision-based strategy. Taking into account these considerations, we propose a modified version of the previously-described model. It is useful to remark that the inclusion of such innovative aspects represents a definitive improvement of our approach w.r.t. the existing literature.

A generic pedestrian  $i$ , besides the set of variables listed in (1), is now characterized also by his/her environmental awareness, described by vector

$$\mathbf{c}_i(t) = \{c_{i,1}(t), c_{i,2}(t), \dots, c_{i,H}(t)\}. \quad (23)$$

Each component  $c_{i,h}$  is associated to one of the possible target destinations: it is set to 1 if pedestrian  $i$  is aware of the presence of the target destination  $h$  and 0 otherwise. A consistent assumption is that all pedestrians initially know at least one possible destination (for example, an individual within a building knows at least the door from which he/she entered). As previously commented, pedestrians may increase their environmental awareness by discovering during motion new points of interest. In mathematical terms, if the position of a previously unknown possible target destination is included, at some instant  $t$ , in the visual region of an individual  $i$ , i.e.,  $\mathbf{x}_h \in \Omega_i^{\text{vis}}(t)$ , the corresponding component  $c_{i,h}$  switches from 0 to 1. We recall that walker gazing direction turns during motion according to Eq. (22) and that it may be partially uncorrelated from the direction of motion. Finally, we reasonably assume that pedestrians remember the location of all discovered destinations long enough to neglect any effect due to memory loss.

Changes in the environment awareness affect pedestrian strategic behavior, which determines the target destination and, ultimately, the preferred component of the velocity, represented by the term  $\mathbf{v}^{\text{targ}}$  in Eq. (9). More in details, a pedestrian  $i$  is constantly allowed to change his/her destination by selecting one of his/her current known points of interest according to a specific decisional rule. A consistent assumption is that pedestrians intend to get out from a building minimizing their efforts, thereby choosing the nearest exit: as a consequence, the target destination  $h_i(t)$  of pedestrian  $i$ , at a given instant  $t$ , is such that

$$\Phi_{h_i(t)}(\mathbf{x}_i(t)) = \min_{h : c_{i,h}(t) \neq 0} \{\Phi_h(\mathbf{x}_i(t))\}, \quad (24)$$

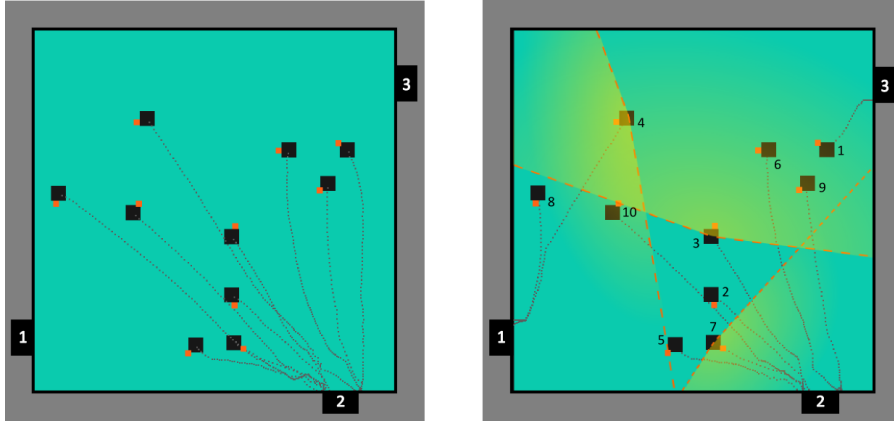


Fig. 8: Effect on pedestrian behavior of an evolving environmental awareness. Left panel: in the absence of a dynamical environmental awareness, all walkers get out from door 2, which is their initial target destination. Right panel: with the inclusion of an evolving environmental awareness, some pedestrians, seeing closer doors, change exit strategy. In both images, pedestrian paths are represented. The black dots indicate the initial position of the walkers, while the orange dots identify their initial gazing direction. In the right panel, the green shadows reproduce the initial visual field of some single pedestrians: each of them is a representative individual of the three types of behavior described in the text.

where  $\Phi_h(\mathbf{x})$  has been already introduced in Section 2.2.1. Finally, the preferred component of the velocity of such an individual  $i$  now reads as follows:

$$\mathbf{v}_i^{\text{targ}}(t) = \bar{v}(s_i(t)) \mathbf{z}_{h_i(t)}(\mathbf{x}_i(t)), \quad (25)$$

where  $\mathbf{z}_{h_i}$  has already been defined in Eq. (14).

## 5 Numerical results - II

In this section, we perform numerical simulations to analyze the role of a dynamical environmental awareness. In all realizations, both physical and behavioral properties of pedestrians are characterized by the same set of assumptions and parameters used in Section 3.1 (in particular,  $R^{\text{rep}} = 1$  m). We here recall that walkers can turn their gazing direction only to align it to the direction of movement (i.e., in order to simplify the picture, we do not consider noises or any other extrapersonal stimuli). Further, each individual is assumed to initially know the location of only one of the possible destinations. This is reasonable as a walker within a building typically is aware, at least, of the position of the entrance from where he/she came in.

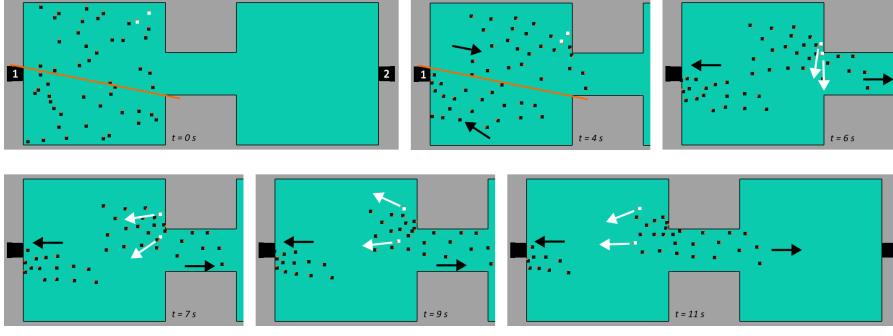


Fig. 9: Crowd dynamics in a building composed of two rooms and a 6 m-wide corridor, in the case of evolving pedestrian environmental awareness. All walkers are initially located in the left room with the same gazing directions given by  $\mathbf{w}_i(0) = (0, 1)$  and are initially aware of door 2 only. Pedestrians below the orange line are able to see door 1, and therefore change their exit strategy, while pedestrians over the orange line move toward the unique exit they know, i.e. door 2. Interestingly, a couple of pedestrians initially placed above the orange line (white dots) sees door 1 during their motion and suddenly changes strategy. The orange dot near each individual indicate his/her gazing direction. Representative images taken at  $t = 0, 4, 6, 7, 9, 11$  seconds.

We first deal with a group of 10 individuals randomly distributed (with a random initial gazing direction) in a square room of  $100 \text{ m}^2$ , with 3 doors located along different walls, see Fig. 8. All pedestrians are initially set to know uniquely the exit located in the bottom side of planimetry of the room, i.e., door 2, which therefore represents the common initial target destination. In mathematical terms, we have that, for any individual  $i = 1, \dots, 10$ ,  $\mathbf{c}_i(0) = \{0, 1, 0\}$  and  $h_i(0) = 2$ . As expected, the inclusion in the model of an evolving environmental awareness completely changes pedestrian collective dynamics, see Fig. 8. A number of walkers in fact no longer get out from the room through door 2 but change evacuation strategy (seeing during their motion the presence of other exits). More specifically, it is possible to observe three different pedestrian behavior:

- some individuals (i.e.,  $i = 1, 4, 8$ ) become aware of the presence of other closer exits and, accordingly, opt to change their target destination;
- some individuals (i.e.,  $i = 3, 5, 6, 9, 10$ ) notice the presence of other exits, but decide to maintain door 2 as target destination, since it is the closest to their position (w.r.t. the known doors);
- some individuals (i.e.,  $i = 2, 7$ ) do not see other exits although such doors may be in the proximity of their position, and therefore maintain their initial target destination.

The rationale of the last phenomenology resides in the specific pedestrian initial gazing direction, and in the following evolution: due to Eq. (22), the

gaze of a pedestrian quickly aligns to his/her direction of motion. However, since the visual field is strongly *anisotropic*, a door may not enter the visual region of a pedestrian even if it is very close to his/her instantaneous position.

For these reasons, it is natural to investigate more deeply the role played by the visual region in the evolution of pedestrian environmental awareness and eventually in overall collective dynamics. For this purpose, we perform a simulation using the “two-rooms-and-a-corridor” planimetry (introduced in Fig. 4). More specifically, a crowd composed of 50 pedestrians is initially randomly distributed in the left room, as shown in the left top panel in Fig. 9. The initial gazing direction of each pedestrian is given by  $\omega_i(0) = \pi/2$  rad, i.e.,  $\mathbf{w}_i(0) = (0, 1)$ , for any  $i$ . We further assume that all individuals are only aware of the the position of the door located in the right room, i.e.,  $\mathbf{c}_i(0) = \{0, 1\}$  and  $h_i(0) = 2$  for any  $i$ . As shown in Fig. 9, pedestrians immediately separate in two groups with opposite moving directions. More specifically, pedestrians initially located in the area below the orange line are able to discover the existence of door 1, as it falls within their visual region. On the contrary, pedestrians that are initially placed over the line quickly align their gazes towards their direction of movements, i.e., towards the right room, thereby loosing the possibility of becoming aware of door 1 (and therefore of getting out through the nearest exit). Interestingly, a couple of individuals initially located in the upper zone (represented by white dots in Fig. 9) are forced by interpersonal repulsive interactions to walk along the wall for a sufficient period, so that door 1 enters their visual region. As a consequence, these walkers change their preferred strategy and exit from the room through door 1 unlike the surrounding pedestrians.

Finally, in order to attest the applicability of our model in more complex and realistic situations, we show a representative numerical result performed on a planimetry of a building constituted of several rooms and provided of 8 exit doors (see Fig. 10). All individuals are characterized by the physical and behavioral parameters listed in Table 1. All of them are initially aware of door 8 only (because for instance they all entered through that door), which therefore represents the common initial target destination, i.e.,  $\mathbf{c}_i(0) = \{0, 0, 0, 0, 0, 0, 0, 1\}$  and  $h_i(0) = 8$  for any  $i = 1, 2, 3$ . Furthermore, gazing direction is randomly generated at initial time for each pedestrian. All individuals enhance their environmental awareness by seeing other exit doors; as a consequence, only pedestrian 1 opts to maintain his/her initial evacuation strategy, because door 8 is the closest to his/her position. Interestingly, walker 2 does not notice the presence of doors 6 and 7, although these are closer exits: this behavior is due to the initial direction of his/her gaze and to the inhibition effect of internal walls that reduce his/her vision region.

## 6 Conclusions

In this paper, a microscopic-discrete mathematical model describing crowd dynamics in no panic conditions has been proposed, based on the concept of



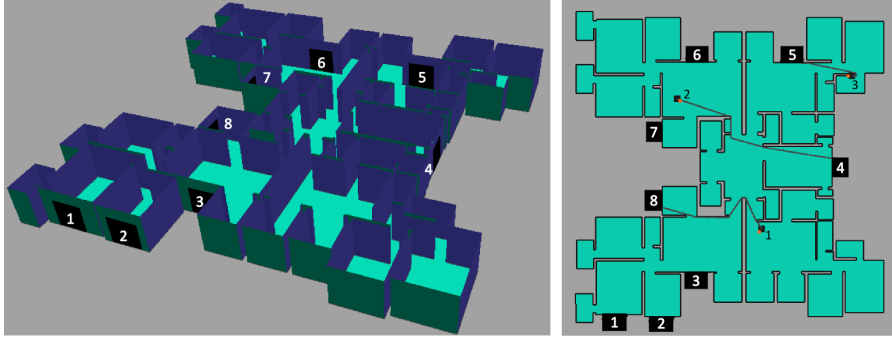


Fig. 10: Crowd dynamics in a building composed of several rooms and exits, in the case of evolving pedestrian environmental awareness. Left panel: three-dimensional view of the building. Right panel: planimetry of the building, with the paths performed by pedestrians. The black dots indicate the initial position of the walkers, whereas the orange dots reproduce the initial direction of their gaze. All pedestrians are initially randomly located within the building with a randomly generated gazing direction. Door 8 is their common initial target destination.

walker *behavioral strategy*. In more detail, in the first modeling setting, each pedestrian has been assumed to move to reach his/her target destination: however, his/her movement is deviated by his/her tendency to remain sufficiently far from walls and from other walkers and by interpersonal physical collisions. These ideas have been translated in a first-order mathematical model based on a set of ODEs, each of them describing the evolution of the velocity of a walker. In particular, the long- and short-range interpersonal interactions introduce non-locality and anisotropy in the individual behavior. Furthermore, pedestrian gazing direction has been assumed to have its own evolution equation. The resulting model has been used to address some specific real-world scenarios involving pedestrian movement in two-dimensional built environments with several structural elements and exits. The simulations presented along the work have been able to capture and characterize the autonomous formation of pedestrian streamlines from the directionally opposite movement of two groups of walkers along a corridor. A simple application of our approach to the optimization of a pedestrian facility in the case of a no panic evacuation has been also proposed. In particular, selected realizations have pointed out that funnel-like constructions facilitate pedestrian evacuation, whereas the presence of columns in the proximity of exits reduces clogging effects.

A key improvement of our mathematical model with respect to the existing discrete-microscopic approaches is that pedestrians have been then allowed to change target destination according to the evolution of their environmental awareness. Such a model component implements the walker ability to evaluate and synthesize the information dynamically acquired about/from the surrounding space. The results of the corresponding numerical simulations have

shown that *evolutionary* behavioral strategies play a fundamental role in capturing realistic crowd phenomenology.

It is useful to remark that our model is based on a vectorial additivity of separate velocity components, each of them describing an environmental influence or a personal strategy. This is of course an approximation, but it is consistent with experimental evidence. As commented in details in [34], quantitative measurements on animals and test persons, subjected to separate or simultaneous stimuli of different nature and strength, show that the individual behavior can be described by a superposition of forces (see [39] [56]): this assumption, in our model, is implemented by a superposition of velocity contributions. The same considerations have allowed Helbing and co-workers to represent pedestrian dynamics as the result of additive social forces. Analogous approaches have been also employed by other authors, see [17] [22] and references therein. For instance, alternative rules for establishing walker behavior can be used: for example, social interactions can be described as gradients of proper dynamically varying fields. Further, individual strategies can be reproduced with evolutionary algorithms [5] [47] or by tools of the game theory [35]. In all these cases, our mathematical modeling environment would require a complete revision. To compute pedestrian velocity, it would be possible also to employ a “constrained optimization” approach. However, some non-trivial issues would arise. In principle, it is not clear whether the optimization should be performed with respect to a single or to multiple objective functions, nor it is evident whether such objective functions should depend upon the actual state of the system, the simulated scenario, the individual interactions or not. The second issue pertains to the optimization constraints. Both the number and the type of constraints should vary according to the specific problem of interest, but it is not evident *a priori* which types of constraints are best-suited to simulate a given situation. Not to mention that the weight associated to each constraint should be carefully chosen, as they significantly affect the simulation outcomes (as much as the model parameters introduced in our present model). Further, introducing in a optimization-based approach a change in pedestrian’s behavior due to an evolving environmental awareness (which is one of the key ingredient of our work) would be quite challenging and should deserve dedicated studies. However, we believe that, for simple scenarios (where the definition of a single objective function is rather straightforward), an optimization-based approach might lead to similar results as the model proposed in this work. For instance, assuming a situation in which each pedestrian wants to leave a location in the shortest time possible, the objective functions of a constrained optimization framework should be defined as the time required to exit the location. In this case, we expect the result of the optimization to be the same as the one presented in our work, as we have defined that the unperturbed velocity of each pedestrian (i.e., without interpersonal interactions) has the same (local) direction of the gradient of the distance function from the target exit. Therefore, the unperturbed trajectory is actually the shortest geodesic path among all possible paths to the target exit, that is the trajectory with the shortest arrival time.

However, the present version of our model can be of course improved in several directions. The interpedestrian collision avoidance, introduced in Eq. (20), is basically a first order version of the term used in the Helbing’s social force model, i.e., a central, exponentially decaying repulsive force. However, few recent works have demonstrated the inability of such a potential to properly describe human collision avoidance, at least in specific density regimes [20], [21], [44], [52], [59], [68]. In particular, in [68], the authors have shown that a more realistic pedestrian microscopic behavior can be reproduced by including a relative velocity in the computation of collision avoidance strategies, at least in second order method frameworks. In this respect, it would be interesting to analyze if such a limitation applies also to our model and, eventually, how this issue can be tackled.

In principle, the present version of the model allows to account the presence in a crowd of different “social groups”. The term “social group” is here used as in [57], i.e., to identify a set of individuals that intentionally walks together since they have social ties, as in the case of friends or family members. To include this feature, it would be only necessary to add a specific attraction/agglomerating term in Eq. (16), to specify the common target destination for the components of each social group, and to further assume that each group member desires to maintain his/her groupmates in his/her visual region during motion (i.e., a corresponding term in the evolution equation of the gazing direction should be introduced). A relevant model refinement would also be the implementation of alternative decision-based strategies, that characterize different categories of pedestrians, i.e., resolute, anxious, and curious, or that may apply to walkers with different travel purposes, i.e., travelers catching a train, commuters in rush hours, shoppers. We in fact recall that in this paper we have always assumed that walkers select as target destination the nearest known point of interest. Further, the realism of the model would increase with the introduction of extrapersonal elements and stimuli that may influence the pedestrian movement and/or perception, such as fog, smoke or specific signage.

As briefly shown by the last simulation setting (cf. Fig. 10), our model has the potential to be employed to describe crowd behavior in more realistic scenarios, which involve an increased number of agents moving in more complex domains. Entering in more details, such model applications may look at the field of crowd management, particularly in relation to sports and stadia events (e.g., test of safe ingress and egress capacities), architectural projects of public and commercial buildings (e.g., optimization of internal structural elements for evacuation procedures) and designs of rail and metro stations (e.g., assessment and improvement of safety, operational integration with large-scale crowd events, evaluation of signage and communication systems). From a modeling point of view, the application of the proposed mathematical approach to one of the above-cited real-world scenarios requires the definition and the comprehensive typology of different kinds of crowds. Possible dimensions that have to be considered are the purpose of the individuals, the level of pedestrian movement (i.e., in terms of velocity and direction), the event/location atmosphere, the identification of possible crowd heterogeneities, the type of interpersonal

interactions, both within the crowd and with external groups (i.e., with stewards or officers). Obviously, a model employment in the case of huge numbers of individuals and/or complex and large enough domains involves computational issues, i.e., mainly related to the optimization of computing time. In this respect, a possible solution is represented by the use of serial and parallel computing. High performance serial computing can be achieved by using the same programming techniques employed in particle fluid-dynamic simulations. Otherwise, parallel computing is possible, for example, using Message Passing paradigm (MPI) or shared memory parallelization. In the first case, the computational domain would be divided in subdomains that in turn would be assigned to a single processor. At each time step, each processor should communicate the pedestrians who leave its portion of domain and enter the sub-domain of a neighboring node. In case of a shared memory parallelization (e.g., on GPU devices), the computational domain and the data structure storing population data would be shared among different threads, each of them updating the state of a sub-set of individuals.

For scenarios characterized by large numbers of individuals, both upscaling and mean-field theory could be convenient strategies to control the high computational effort required by reproducing the pedestrian flow in extended environments, as provided by the relative literature, see for relevant examples [6] [16] [17] [19] [42] and references therein. However, these approaches would cause the loss of the characterization of the single pedestrians, i.e., in particular of the individual gazing direction and environmental awareness (which, as already explained, are key features of our model). Entering in more details, both continuous and kinetic methods can take into account the existence of a vision region: however, it is aligned to the direction of the desired velocity, i.e., pedestrian head is assumed to be always directed toward the target objective, see [13] [14]. In this respect, without the inclusion of a proper (possibly uncoupled) evolution law for the gaze of each pedestrian, it would be not possible to reproduce dynamical variations of the individual environmental awareness which, as seen, result in realistic decision-based behavior.

Finally, it is fundamental to remark that most of those applications related to safety problems involve panic situations. This topic, out of the scope of the present work, would involve significant modeling changes, i.e., both in determining the individual paths towards the target destination and in dealing with the interpersonal interactions. As it is widely known from the phenomenological literature [16], [26], pedestrians entering a panic state in fact tend to chaotically follow other individuals, thereby clustering into more or less large groups and dropping their specific destination. Moreover, interactions with walls and obstacles follows completely different rules, since panicked walkers not only care less about obstacles but may prefer to approach walls for safety reasons (especially in low visibility situations). For these reasons, a realistic model should also include reasonable laws for the transition of each pedestrian from a normal condition to a panic scenario.

## Appendix: parameter estimate and sensitivity analysis

As already explained, the model parameters can be distinguished in physical quantities and merely technical coefficients. When possible, we opt to use a parameter estimate inferred from the existing literature. In the other cases, our choice is done after preliminary simulations, that help us to select the more realistic parameter setting. In this respect, this Appendix gives details both on how we establish the set of parameter values and on how our estimates affect the simulation outcomes.

*Variation of the visual region extension.* Although the physical significance of both  $R_i^{\text{vis}}$  and  $\theta_i$  is sufficient to define their values, it is worth noting that the extension of the visual region can definitely change pedestrian behavior. In order to analyze this aspect, we refer to the simulation setting of Fig. 8 in Section 5, i.e., a group of 10 individuals distributed in a square room with three exits that want to reach the nearest door. In particular, all pedestrians are set to initially know only the position of exit 2 but have a variable environmental awareness (i.e., each of them is allowed to opt for an alternative door if he/she actually sees it). Keeping fixed the other model parameters, we vary either the visual depth  $R_i^{\text{vis}} = R^{\text{vis}}$  and the visual angle  $\theta_i = \theta$  (we recall that both are in common for all individuals). As captured by the trajectories reported in Fig. 11, very low values of  $R^{\text{vis}}$  and  $\theta$  result in a significantly limited visual region for the pedestrians, that therefore typically maintain door 2 as target destination (they are in fact not able to see any other exits). The model outcomes in such a range of parameters could be also obtained by employing a discrete approach that does not include a variable environmental awareness. The capability of pedestrians to individuate (and therefore to choose) alternative targets then increases with the overall extension of their visual region, i.e., it is enhanced by increments in the values of  $R^{\text{vis}}$  and  $\theta$ . In particular, for any  $R^{\text{vis}}$  higher than the size of the domain, the walker behavior is entirely determined by the extension of his/her visual angle  $\theta$ , see the right panels in Fig. 11. Given these considerations, we opt to estimate  $R^{\text{vis}} = 50$  m, which is in the range of the characteristic dimensions of the domains employed in this work, and  $\theta = 85^\circ$ , a value consistent with the literature, see [11].

For the sensitivity analysis of the remaining model parameters, we hereafter employ the “two-adjacent-rooms-without-column” domain presented in Section 3.3 (cf. Fig. 7 (top-right panel)). In particular, a group of 200 individuals is initially located in the left room and wants to reach the door placed in the right room. Starting from the very same initial distribution of pedestrians, we then singularly vary selected model parameters and analyze the corresponding simulation outcomes both by monitoring the evacuation time of the crowd and by observing the emergence of characteristic collective dynamics.

*Variation of the wall repulsion parameters.* The wall repulsion radius  $R^{\text{wall}}$  is estimated on the basis of empirical considerations. We first assume that a person within a building takes into account the presence of a wall only when he/she is approaching it. In this respect, given  $R^{\text{body}} = 0.3$  m, we set

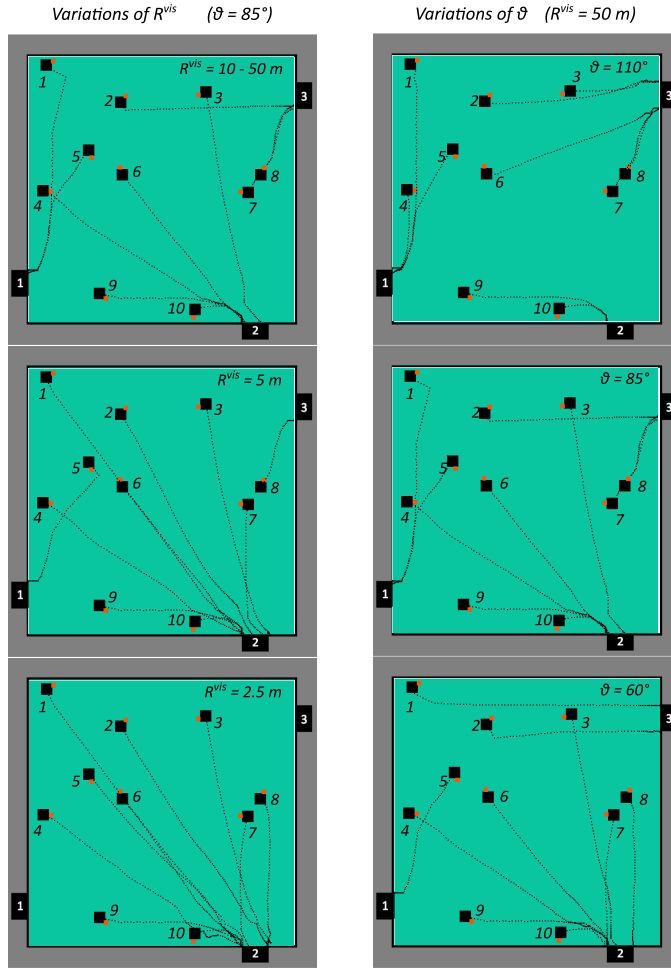


Fig. 11: Effect of the extension of the visual region on pedestrian dynamics. The initial distribution of the group of individuals is the same for all realizations. All walkers initially know only the position of door 2, but they have an evolving environmental awareness (i.e., they are allowed to opt for the nearest known door).

$R^{\text{wall}} = 0.4$  m, i.e., an individual tries to maintain a distance of about  $R^{\text{wall}} - R^{\text{body}} = 0.1$  m from the nearest wall. Lower values of  $R^{\text{wall}}$  would result in fact in decrements of the evacuation time (see the corresponding panel in Fig. 12) but also in unphysical dynamics: the pedestrians would be in fact dramatically pressed along the domain boundary or along the internal walls. On the opposite, for  $R^{\text{wall}} > 0.4$  m, no variations in the evacuation time occur. This is a further justification for the chosen parameter value. The coefficients  $A$  and  $B$  determine instead the exact form of the exponential function that

defines the wall repulsion velocity. Keeping all the other parameters fixed,  $A$  does not have a significant impact on the overall dynamics, see Fig. 12: indeed, we opt for an intermediate value  $A = 1$  m/s. Variations of  $B$  play instead a critical role in the model outcomes. For  $B < 10^{-2}$  m, the evacuation time is almost constant: however, it decreases when  $B \in (10^{-2} \text{ m}, 1 \text{ m})$ , until reaching a threshold for  $B > 1$  m. However, high enough values of  $B$  (i.e.,  $> 1$  m) correspond to the unrealistic situation of pedestrians that constantly move along the boundary of the domain (not shown). We indeed opt to set  $B = 10^{-2}$  m.

*Variation of the interpersonal interaction parameters.* By setting the pedestrian body radius  $R^{\text{body}}$  equal to 0.3 m, the contact radius  $R^{\text{cont}}$  is necessarily equal to  $2R^{\text{body}} = 0.6$  m for any pair of interacting pedestrians. The evacuation time of the crowd decreases for  $C \in (10^{-1} \text{ s}^{-1}, 30 \text{ s}^{-1})$ , see Fig. 12. However, we observe that, for too low values (i.e.,  $< 5 \text{ s}^{-1}$ ), the walkers collide too frequently. On the opposite, high enough values of  $C$  (i.e.,  $> 30 \text{ s}^{-1}$ ) result in unrealistically dynamics, as the pedestrians “rebound” one on each other (due to the too high contribution of the contact component of the velocity) thereby barely reaching the target door. Given such considerations, we estimate  $C$  equal to  $25 \text{ s}^{-1}$ . The evacuation time has instead a biphasic behavior with respect to variations of  $D$ , as it is constant for  $D < 10 \text{ s}^{-1}$ , increases for  $D \in (10 \text{ s}^{-1}, 10^3 \text{ s}^{-1})$ , until reaching a threshold for  $D > 10^3 \text{ s}^{-1}$ . In this respect, we opt for the intermediate estimate  $D = 50 \text{ s}^{-1}$ .

The interpersonal repulsion radius is not determined by pedestrian physical characteristics (unless the reasonable conditions  $R^{\text{cont}} < R^{\text{rep}} < R^{\text{vis}}$ ). It in fact defines the minimal distance below which a walker starts to deviate his/her motion to avoid possible collisions with another individual, i.e., it has a sort of psychological nature. In particular, the top-central panel in Fig. 12 shows that variations of  $R^{\text{rep}}$  within the above-cited range of values do not significantly affect the simulation outcomes (in terms of evacuation time of the crowd). However, from a phenomenological point of view, it is clear that the comfort interpersonal distance, evaluated by  $R^{\text{rep}}$  depends on the specific situation. In this respect, it is consistent to assume  $R^{\text{rep}} = 1$  m in the case of evacuation scenarios (as panicking individuals tend to remain close one to another) and a higher  $R^{\text{rep}} = 3$  m in the other cases. The coefficient  $E$  does not affect the dynamics of the crowd within a given range of values (i.e.,  $E < 1$  m/s, see again Fig. 12). However, outside such a set of values, i.e., for  $E$  high enough, we observe a blow up in the evacuation time: this is due to the fact that the repulsive component overcomes the target velocity  $\mathbf{v}^{\text{targ}}$  and therefore the individuals try to keep the desired interpersonal distance rather than to reach the exit door. Given these observations, we opt for  $E = 1$  m/s. On the opposite, variations of  $F$  do not play a critical role in walker behavior (refer to Fig. 12 (bottom-central graph)): indeed, an intermediate  $F = 0.5$  m is chosen.

*Variation of the gazing evolution parameter.* The estimate of coefficient  $G$  is inferred by qualitative and physical observations: too low values of  $G$  (i.e.,  $< 1$  (rad s)/m) generate unacceptable extremely rapid and uncontrollable

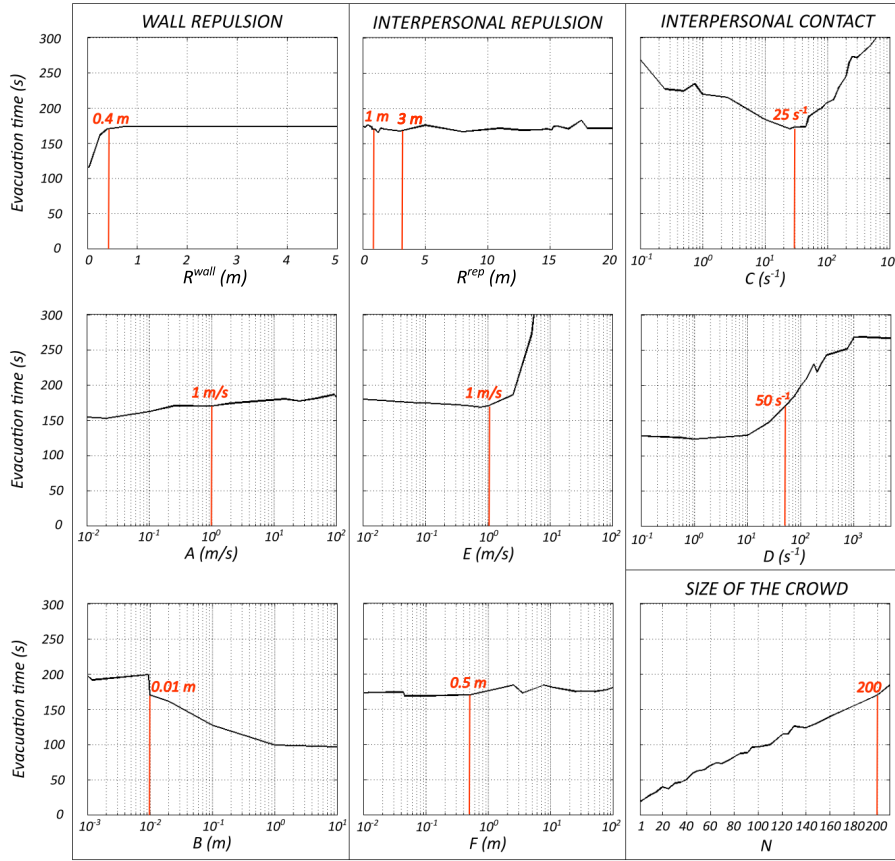


Fig. 12: Effect of variations of selected model parameters. The graphs are obtained by monitoring the evacuation time in the case of the “two-adjacent-rooms-without-column” simulation setting. In all cases the initial pedestrian distribution is the same. Within each panel, we identify the parameter estimate used in the previous sections.

rotations of pedestrian’s head (not shown). On the opposite, too high values (i.e.,  $> 3$  (rad s)/m) obviously force each walker to perfectly align his/her gaze to his/her direction of motion, which is unrealistic. We indeed set an intermediate  $G = 2$  (rad s)/m.

*Variation of the number of pedestrians.* The number of pedestrian dramatically affects the dynamics of the system. As reproduced in Fig. 12 (bottom-right panel), aside slight perturbations due to numerical effects, the evacuation time is in fact directly proportional to the number of individuals  $N$ . In this respect,  $N = 200$  corresponds to a value that allows to have a reasonable pedestrian density, i.e., of 1 individual/m<sup>2</sup>, in the case of the domain setting used for this



parameter sensitivity. The same considerations hold for the number of walker used in the simulations presented in the previous sections.

Summing up the sensitivity analysis proposed in this section, it is possible to conclude that pedestrian behavior strongly depends both on the extension and on the dynamics of the visual region (which are defined by the visual depth/angle and by the coefficient  $G$ , respectively). However, empirical considerations allow us to infer a consistent estimate of the values of such parameters. On the opposite, the wall repulsion radius, as well as the interpersonal repulsion distance, does not affect the model outcomes. The rationale is that the corresponding velocity contributions are negative exponential functions: indeed, rather than the point at which a pedestrian *starts* to experience interpersonal interactions, it is fundamental the exact form of the exponential laws, given by the relative coefficients  $(A, B, C, D, E, F)$ . However, physical observations help us to provide a realistic set also of these parameters. Finally, the overall simulation results are obviously affected by the total number of individuals taken into account, that obviously determines the evacuation time of the overall crowd. In this respect, it is necessary to account a realistic density of pedestrians for unit of area (i.e.,  $\approx 1 \text{ m}^{-2}$ ).

**Acknowledgements** The authors want to thank Prof. Luigi Preziosi for fruitful discussions.

## References

1. Alt H., Welzl, E., 1988. Visibility graphs and obstacle-avoiding shortest paths. *Zeitschrift für Operations Research*, 32 (3-4), 145 – 164
2. Appert-Rolland, C., Cividini, J., Hilhorst, H. J., Degond, P., 2014. Pedestrian flows: From individuals to crowds. *Transportation Research Procedia*, 2, 468 - 476
3. Ashford, N., O’Leary, M., McGinity, P. D., 1976. Stochastic modelling of passenger and baggage flows through an airport terminal. *Traffic Engineering and Control*, 17, 207 – 210
4. Batty, M., 1997. Predicting where we walk. *Nature*, 388, 19 – 20
5. Baeck, T., 1996. *Evolutionary Algorithms in Theory and Practice*. Oxford University Press, New York.
6. Bellomo, N., Dogbé, C., 2008. On the modelling crowd dynamics from scaling to hyperbolic macroscopic models. *Math. Models Methods Appl. Sci.*, 18 (suppl.), 1317 – 1345
7. Bellomo, N., 2008. Modeling Complex Living Systems – A Kinetic Theory and Stochastic Game Approach. In *Modeling and Simulation in Science, Engineering and Technology*, Birkhäuser
8. Bellomo, N., Bellouquid, A., 2010. On the modeling of vehicular traffic and crowds by kinetic theory of active particles. In *Mathematical Modeling of Collective Behavior in Socio-Economic and Life Sciences*, Eds. G. Naldi, L. Pareschi and G. Toscani, Modeling and Simulation in Science, Engineering and Technology, Birkhäuser, pp. 273 – 296.
9. Bellomo, N., Bellouquid, A., 2011. On the modeling of crowd dynamics: Looking at the beautiful shapes of swarms. *Netw. Heterog. Media*, 6, 383 – 399.
10. Bellouquid, A., De Angelis, E., Fermo, L., 2012. Towards the modeling of vehicular traffic as a complex system: A kinetic theory approach. *Math. Models Methods Appl. Sci.*, 22, 1140003
11. Bruno, L., Tosin, A., Tricerri, P., Venuti, F., 2011. Non-local first-order modelling of crowd dynamics: a multidimensional framework with applications. *Appl. Math. Model.*, 35 (1), 426 – 445.

12. Burstedde, C., Klauck, K., Schadschneider, A., Zittartz, J., 2001. Simulation of pedestrian dynamics using a two-dimensional cellular automaton. *Physica A*, 295 (4), 507 – 525
13. Carrillo, J. A., D’Orsogna, M. R., Panferov, V., 2009. Double milling in self-propelled swarms from kinetic theory. *Kinet. Relat. Models*, 2 (2), 363 – 378
14. Carrillo, J. A., Fornasier, M., Toscani, G., Vecil, F., 2010. Particle, kinetic, and hydrodynamic models of swarming. In *Mathematical Modeling of Collective Behavior in Socio-Economic and Life Sciences*, Eds. G. Naldi, L. Pareschi and G. Toscani, Modeling and Simulation in Science, Engineering and Technology, Birkhäuser, pp. 297 – 336
15. Carstens, R. L., Ring, S. L., 1970. Pedestrian capacities of shelter entrances. *Traffic Engineering*, 41, 38 – 43
16. Colombo, R. M., Rosini, M. D., 2005. Pedestrian flows and non-classical shocks. *Math. Methods Appl. Sci.*, 28 (13), 1553 – 1567
17. Coscia, V., Canavesio, C., 2008. First-order macroscopic modelling of human crowd dynamics. *Math. Models Methods Appl. Sci.*, 18 (suppl.), 1217 – 1247
18. Cristiani, E., Piccoli, B., Tosin, A., 2011. Multiscale Modeling of Granular Flows with Application to Crowd Dynamics. *Multiscale Model. Simul.*, 9 (1), 155 – 182
19. Cristiani, E., Piccoli, B., Tosin, A., 2014. *Multiscale Modeling of Pedestrian Dynamics. MS and A: Modeling, Simulation and Applications*, vol. 12, Springer International Publishing
20. Curtis, S., Manocha, D., 2014. Pedestrian simulation using geometric reasoning in velocity space. In *Pedestrian and Evacuation Dynamics 2012*, pp 875 – 890, Springer.
21. Curtis, S., Zafar, B., Gutub, A., Manocha, D., 2012. Right of way. *The Visual Computer*, 1 – 16
22. Dogbé, C., 2010. Mathematical and Computer modelling, 52, 1506 – 1520
23. Drasdo, D., 2005. On selected individual-based approaches to the dynamics of multicellular systems. In *Multiscale Modeling*, Eds. W. Alt and M. Griebel, Birkhäuser, pp. 169 – 203.
24. Garbrecht, D., 1973. Describing pedestrian and car trips by transition matrices. *Traffic Quarterly*, 27, 89 – 109
25. Hankin, B. D., Wright, R. A., 1958. Passenger flow in subways. *Operational Research Quarterly*, 9, 81 – 88
26. Helbing, D., Johansson, A., Al-Abideen, H. Z., 2007. Dynamics of crowd disasters: an empirical study. *Physical Review E*, 75 (4), 0406109
27. Helbing, D., Molnar, P., 1995. Social force model for pedestrian dynamics. *Physical Review E*, 51, 4282 – 4286
28. Helbing, D., 1992. A fluid-dynamic model for the movement of pedestrians. *Complex Systems*, 6, 391 – 415
29. Helbing, D., Molnar, P., Farkas, I. J., Bolay, K., 2001. Self-organizing pedestrian movement. *Environment and Planning B: Planning and Design*, 28, 361 – 383
30. Helbing, D., 1998. Pedestrian dynamics and trail formation. In *Traffic and Granular Flow '97*, Eds. M. Schreckenberg and D. E. Wolf, Springer, Berlin, pp 21 – 36
31. Helbing, D., Molnar, P., 1997. Self-organization phenomena in pedestrian crowds. In *Self-organization of Complex Structures: From Individual to Collective Dynamics*, Ed. F. Schweitzer, Gordon and Breach, London, pp 569 – 577
32. Helbing, D., Vicsek, T., 1999. Optimal self-organization. *New Journal of Physics*, 1, 13.1 – 13.17
33. Helbing, D., Molnar, P., Schweitzer, F., 1994. Computer simulations of pedestrian dynamics and trail formation. *Evolution of Natural Structures*, 229 – 234
34. Helbing, D., Farkas, I. J., Molnar, P., Vicsek, T., 2002. Simulation of pedestrian crowds in normal and evacuation situations. *Pedestrian and evacuation dynamics*, 21, 21 – 58
35. Helbing, D., 1996. A stochastic behavioral model and a microscopic foundation of evolutionary game theory. *Theory and Decision* 40, 149 – 179
36. Henderson, L. F., 1971. The statistics of crowd fluids. *Nature*, 229, 381 – 383
37. Henderson, L. F., 1974. On the fluid mechanics of human crowd motion. *Transportation Research*, 8, 509 – 515
38. Henderson, L. F., Jenkins, D. M., 1973. Response of pedestrians to traffic challenge. *Transportation Research*, 8, 71 – 74

39. Herkner, W. H., 1975. Ein erweitertes Modell des Appetenz-Aversions-Konflikts. *Z. Klin. Psychol.*, 4, 50 – 60
40. Hill, M. R., 1984. *Walking, Crossing Streets, and Choosing Pedestrian Routes*. University of Nebraska Press, Lincoln, NE
41. Hoogendoorn, S., Daamen, W., 2005. Pedestrian Behavior at Bottlenecks. *Transportation Science*, 39, 147 – 159
42. Hughes, R. L., 2002. A continuum theory for the flow of pedestrians. *Transport. Res. B*, 36 (6), 507 – 535
43. Isobe, M., Helbing, D., and Nagatani, T., 2004. Experiment, theory, and simulation of the evacuation of a room without visibility. *Physical Review E*, 69, 066132
44. Karamouzas, I., Skinner, B., Guy, S. J., 2014. Universal power law governing pedestrian interactions. *Physical Review Letters*, 113 (23), 238701
45. Kimmel, R., and Sethian, J.A., 1996. Fast Marching Methods for Computing Distance Maps and Shortest Paths. CPAM Report 669, Univ. of California, Berkeley.
46. Kimmel, R., and Sethian, J.A., 1998. Fast Marching Methods on Triangulated Domains. *Proc Nat Acad Sci*, 95, 8341 – 8435
47. Klockgether, J., Schwefel, H. P., 1970. Two-phase nozzle and hollow core jet experiments. In *Proceedings of the Eleventh Symposium on Engineering Aspects of Magneto Hydrodynamics*, Ed. D. G. Elliott, pp. 141 – 48
48. Krause, J., Ruxton, G. D., 2002. *Living in Groups*. Oxford University Press, Oxford
49. Kretz, T., Grunebohm, A., Schreckenberg, M., 2006. Experimental study of pedestrian flow through a bottleneck. *Journal of Statistical Mechanics: Theory and Experiments*, P10014
50. Kretz, T., Grunebohm, A., Kaufman, M., Mazur, F., Schreckenberg, M., 2006. Experimental study of pedestrian counterflow in a corridor. *Journal of Statistical Mechanics: Theory and Experiments*, P10001
51. Kretz, T., 2009. Pedestrian traffic: on the quickest path. *Journal of Statistical Mechanics: Theory and Experiment*. 2009 (03), P03012.
52. Lämmel, G., Plaue, M., 2012. Getting out of the way: Collision avoiding pedestrian models compared to the real world. *Pedestrian and Evacuation Dynamics*, pp 1275 – 1289
53. Lovas, G. G., 1994. Modelling and simulation of pedestrian traffic flow. *Transportation Research B*, 28, 429 – 443
54. Maury B., Venel, J., 2008. A mathematical framework for a crowd motion model. *C. R. Math. Acad. Sci. Paris*, 346 (23-24), 1245 – 1250
55. Mayne, A. J., 1954. Some further results in the theory of pedestrians and road traffic. *Biometrika*, 41, 375 – 389
56. Miller, N. E., 1944. Experimental studies of conflict. In *Personality and the behavior disorders*, Vol. 1, Ed. J. McV. Hunt, Ronald, New York.
57. Moussaid, M., Perozo, N., Garnier, S., Helbing, D., Theraulaz, G., 2010. The walking behaviour of pedestrian social groups and its impact on crowd dynamics. *PloS one*, 5, e10047
58. Navin, P. D., Wheeler, R. J., 1969. Pedestrian flow characteristics. *Traffic Engineering*, 39, 31 – 36
59. Ondřej, O., Pettré, J., Olivier, A. H., Donikian, S., 2010. A synthetic-vision based steering approach for crowd simulation. *ACM Transactions on Graphics (TOG)*, 29 (4), 123.
60. Roy, J. R., 1992. Queuing in spatially dispersed public facilities. Paper presented at the Fourth World Congress of the Regional Science Association International, Palma de Mallorca.
61. Schadschneider, A., Klingsch, W., Klüpfel, H., Kretz, T., Rogsch, C., Seyfried, A., 2009. Evacuation Dynamics: Empirical Results, Modeling and Applications. *Encyclopedia of Complexity and Systems Science*, pp 3142 – 3176.
62. Scianna, M., Preziosi, L., 2012. Multiscale developments of the cellular Potts model. *Multiscale Model Simul.*, 10 (2), 342 – 382.
63. Seyfried, A., Steffen, B., Flingsch, W., Boltes, M., 2005. The fundamental diagram of pedestrian movement revisited. *J. Stat. Mech. Theory Exp.*, 2005 (P10002), 1 – 13.
64. Timmermans, H., Van der Hagen, X., Borgers, A., 1992. Transportation systems, retail environments and pedestrian trip chaining behaviour: modelling issues and applications. *Transportation Research B*, 26, 45 – 59.

- 
65. Yu, W., Johansson, A., 2007. Modeling crowd turbulence by many-particle simulations. *Physical Review E*, 76, 046105.
  66. Yuhaski, S. J. Jr., Macgregor Smith, J., 1989. Modelling circulation systems in buildings using state dependent queueing models. *Queueing Systems*, 4, 319 – 338
  67. Venuti, F., Bruno, L., 2007. An interpretative model of the pedestrian fundamental relation. *C. R. Mecanique*, 335 (4), 194 – 200.
  68. Zanlungo, F., Ikeda, T., Kanda, T., 2011. Social force model with explicit collision prediction. *EPL (Europhysics Letters)*, 93 (6), 68005.